

many more assumptions than the first (e.g., rotational barriers in the starting species and frequencies of the vibrational modes in **3**), is rather long and involved, and is not reported in detail here. This second calculation is in general agreement with the first and gives $\log A = 10$.

Thus, according to both calculations, the preexponential for the reaction outlined in Scheme VI is approximately $\log A = 11$

± 1 . Since it is much larger than the experimental value ($\log A = 6.4$) for the high-temperature reaction, we conclude that it is unlikely that this reaction occurs by the unimolecular mechanism A (Scheme III).

Registry No. Ag(110), 7440-22-4; *tert*-butyl alcohol, 75-65-0; isobutylene oxide, 558-30-5; deuterium, 7782-39-0.

Gas-Phase Acidities of Organosilanes and Electron Affinities of Organosilyl Radicals

Donna M. Wetzel, Karen E. Salomon, Susan Berger, and John I. Brauman*

Contribution from the Department of Chemistry, Stanford University, Stanford, California 94305-5080. Received May 20, 1988

Abstract: We have measured the equilibrium gas-phase acidities for a series of alkyl- and aryl-substituted organosilanes, and the cross sections for electron photodetachment of the corresponding conjugate bases, using ion cyclotron resonance spectrometry. Gas-phase acidities for the conjugate acids of these compounds are $\Delta H^\circ_{\text{acid}}(\text{SiH}_4) = 372.8 \pm 2$ kcal/mol, $\Delta H^\circ_{\text{acid}}(\text{C}_6\text{H}_5\text{SiH}_3) = 370.7 \pm 2$ kcal/mol, $\Delta H^\circ_{\text{acid}}(\text{C}_6\text{H}_5(\text{CH}_3)\text{SiH}_2) = 374.2 \pm 2$ kcal/mol, $\Delta H^\circ_{\text{acid}}(\text{CH}_3\text{SiH}_3) = 378.3 \pm 2$ kcal/mol, and $\Delta H^\circ_{\text{acid}}((\text{CH}_3)_3\text{SiH}) \geq 382.8 \pm 2$ kcal/mol. The electron affinities are $\text{EA}(\text{SiH}_3^*) = 32.4 \pm 0.6$ kcal/mol, $\text{EA}(\text{C}_6\text{H}_5\text{SiH}_2^*) = 33.1 \pm 0.1$ kcal/mol, $\text{EA}(\text{C}_6\text{H}_5(\text{CH}_3)\text{SiH}^*) = 30.7 \pm 0.9$ kcal/mol, $\text{EA}(\text{CH}_3\text{SiH}_2^*) = 27.5 \pm 0.8$ kcal/mol, and $\text{EA}((\text{CH}_3)_3\text{Si}^*) = 22.4 \pm 0.6$ kcal/mol. These values were used to determine the Si-H bond dissociation energies in the organosilicon hydrides: $D^\circ[\text{SiH}_3\text{-H}] = 91.6 \pm 2$ kcal/mol, $D^\circ[\text{C}_6\text{H}_5\text{SiH}_2\text{-H}] = 90.2 \pm 2$ kcal/mol, $D^\circ[\text{C}_6\text{H}_5(\text{CH}_3)\text{SiH-H}] = 91.3 \pm 3$ kcal/mol, $D^\circ[\text{CH}_3\text{SiH}_2\text{-H}] = 92.2 \pm 3$ kcal/mol, and $D^\circ[(\text{CH}_3)_3\text{Si-H}] \geq 91.0 \pm 2$ kcal/mol. The electronic structure of the organosilicon compounds studied is discussed and compared with that in the corresponding carbon compounds.

Thermochemical properties are indispensable tools for understanding chemical reactivity and making predictions about intermediates, products, equilibria, and reaction mechanisms. It is surprising, therefore, that despite the prolific investigation and utilization of organosilicon chemistry in the past 20 years, thermochemical data for organosilicon compounds remain scarce. For example, the data base of ionic, gas-phase thermochemical measurements¹ which has grown impressively in recent years has only minimal coverage in other classes such as organometallics. Especially important, yet experimentally challenging, are thermochemical measurements involving reactive silicon intermediates² such as divalent silicon compounds, silyl radicals, cations, and anions. In this paper, we report our measurements of the gas-phase acidities of selected organosilanes and the electron affinities of the corresponding organosilyl radicals.

In addition to contributing thermochemical data, gas-phase investigations involving equilibrium basicities and electron photodetachment spectroscopy of silyl and substituted silyl anions can provide information about substituent effects, hybridization, and electronic structure. This information, well known for carbon

compounds, is largely unavailable for organosilicon anions and radicals. Additional motivation for our experiments was the possibility of detailed comparisons between the behavior of silicon and carbon in anions and radicals.

Recent gas-phase investigations have contributed significantly to the understanding of silicon compound reactivity. Of particular interest are the studies involving negative ion-molecule reactions of silicon compounds.³ Many important features of nucleophilic substitution reactions have been identified, with concomitant discovery of novel methods for generating a wide variety of organic anions and demonstration of stable pentavalent silicon anions. These studies have revealed excellent correspondence between reactivity patterns of silicon compounds in gas and condensed phases. Thus, the information gained on the behavior of gas-phase organosilyl anions, radicals, and neutral hydrides may enable direct correlation to solution-phase organosilicon chemistry.

We have measured the equilibrium constants for proton-transfer reactions between organosilanes (alkyl- and aryl-substituted silanes) and alcohols (alkoxide ions), from which the organosilane acidities can be determined. Gas-phase equilibrium measurements have been reported⁴ only for SiH_4 . Very recently, Damrauer, Kass, and DePuy⁵ have reported gas-phase organosilane acidities, obtained from bracketing experiments performed in a flowing afterglow apparatus. The elegant design of the bracketing experiments allowed determination of both Si-H and C-H acidities. Our equilibrium results are generally in good agreement.

We have also measured the electron photodetachment cross sections for the corresponding organosilyl anions (conjugate bases). The only reported detachment data on organosilyl anions are

(1) Compilations include: (a) Bartmess, J. E.; McIver, R. T., Jr. In *Gas Phase Ion Chemistry*; Bowers, M. T., Ed.; Academic: New York, 1979; Vol. 2. (b) Drzagic, P. S.; Marks J.; Brauman, J. I. In *Gas Phase Ion Chemistry*; Bowers, M. T., Ed.; Academic: Orlando, FL, 1984; Vol. 3. (c) Kebarle, P.; Chowdhury, S. *Chem. Rev.* **1987**, *87*, 513.

(2) General reviews of some silicon reaction intermediates: (a) Raabe, G.; Michl, J. *Chem. Rev.* **1985**, *85*, 419. (b) Bertrand, G.; Trinquier, G.; Mazerolles, P. In *Organometallic Chemistry Reviews*; Seyferth, D., Davies, A. G., Fischer, E. O., Normant, J. F., Reutov, O. A., Eds. *J. Organomet. Library*, 12; Elsevier Scientific Publishing Co.: New York, 1981. (c) Wiberg, N. *J. Organomet. Chem.* **1984**, *273*, 141. (d) Gusel'nikov, L. E.; Nametkin, N. S. *Chem. Rev.* **1979**, *79*, 529. (e) Gaspar, P. P. In *Reaction Intermediates*; Plenum Press: New York, 1980, 1981, and 1985. (f) West, R. *Pure Appl. Chem.* **1984**, *56*, 163. (g) Brook, A. G.; Baines, K. M. *Adv. Organomet. Chem.* **1986**, *25*, 1. (h) West, R. *Angew. Chem., Int. Ed. Engl.* **1987**, *26*, 1201. (i) Gaspar, P. P.; Holten, D.; Konieczny, S.; Corey, J. Y. *Acc. Chem. Res.* **1987**, *20*, 329.

(3) DePuy, C. H.; Damrauer, R.; Bowie, J. H.; Sheldon, J. C. *Acc. Chem. Res.* **1987**, *20*, 127.

(4) Bartmess, J. E.; Scott, J. A.; McIver, R. T., Jr. *J. Am. Chem. Soc.* **1979**, *101*, 6047.

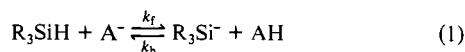
(5) Damrauer, R.; Kass, S. R.; DePuy, C. H. *Organometallics* **1988**, *7*, 637.

experiments involving SiH_3^- : photodetachment studies by Reed and Brauman⁶ and photoelectron studies by Nimlos and Ellison.⁷

From the resulting acidities and electron affinities we have derived Si-H bond dissociation energies, which compare well to the bond dissociation energies measured previously by Walsh.⁸ The thermochemical data are presented with a discussion of the substituent effects and energetics. Comparisons to the analogous carbon compounds show interesting differences in electronic structure between carbon and silicon compounds.

Experimental Section

General. The data reported in this study were obtained from two types of experiments: gas-phase equilibria and electron photodetachment spectroscopy. In the first type of experiment, equilibrium was set up between two acids (the organosilane acid and an appropriate reference acid, AH) and their conjugate bases, as shown in the equation:



By monitoring time-dependent or equilibrium abundances of the conjugate bases involved, the equilibrium constant for the proton-transfer reaction was obtained. In the photodetachment spectroscopy experiments, anions were generated and irradiated continuously. By monitoring the abundance of the anion as a function of photon wavelength, a cross section for electron photodetachment, shown in eq 2, was obtained.

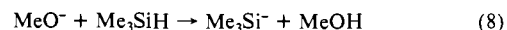
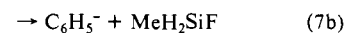
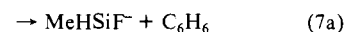
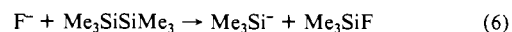
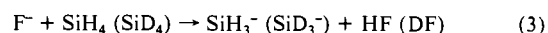


Gas-phase anions in both types of experiments were generated, trapped, and detected using ion cyclotron resonance (ICR) spectrometry. Detection circuitry incorporated single-frequency phase-sensitive detection and a capacitance bridge^{9,10} to measure the ion concentrations. Data acquisition methods, as detailed below, differed for the two types of measurements, but the ion-molecule reactions used to generate the anions were the same.

Materials. The parent neutral molecules and reference acids not synthesized were used as received (unless otherwise noted here) followed by degassing via several freeze-pump-thaw cycles. They were obtained from the following sources: nitrogen trifluoride (NF_3) from Ozark-Mahoning; silane (SiH_4), methylsilane (MeSiH_3), trimethylsilane (Me_3SiH), hexamethyldisilane ($\text{Me}_3\text{SiSiMe}_3$), 1,1,2-trimethyldisilane ($\text{Me}_2\text{HSiSiH}_2\text{Me}$), phenylmethylsilane (PhMeSiH_2), phenylsilane (PhSiH_3) from Petrarch; methanol (CH_3OH), isopropyl alcohol (*i*-PrOH) from Baker Chemical; 3,3-dimethyl-2-butanol (*t*-BuC(Me)-HOH), 2,2-dimethyl-3-pentanol (*t*-BuC(Et)HOH) from Aldrich; and 2,2,4-trimethyl-3-pentanol (*t*-BuC(*i*-Pr)HOH) from Wiley Organics.

Some of the parent neutral molecules were synthesized. Silane- d_4 (SiD_4), prepared by reaction¹¹ of LiAlD_4 with SiCl_4 , was purified by four successive passes through -130°C traps. Phenylsilane- d_3 (PhSiD_3), prepared by an analogous method from phenyltrichlorosilane,¹² was purified from the reaction mixture by two distillations under reduced pressure. Isotopic purity of both deuterium compounds were verified by GCMS (Hewlett-Packard, Model 5995, SE-30 column). Dimethyl peroxide (MeOOME) was prepared by an adaptation of the established procedure of Hanst and Calvert¹³ and purified by transfer through a -78°C trap. It was necessary to purify PhSiH_3 , PhMeSiH_2 , and $\text{Me}_2\text{HSiSiH}_2\text{Me}$ using gas chromatography on an SE-30 column. MeSiH_3 and Me_3SiH were purified by bulb-to-bulb distillation prior to the equilibrium measurements.

Ion Generation. Gas-phase organosilyl anions were prepared using ion-molecule reactions involving either proton transfer or nucleophilic displacement reactions. Primary ions MeO^- and F^- (generated from dissociative electron capture on MeOOME and NF_3 , respectively) reacted with the appropriate neutrals as shown in eq 3-9.



The neutral organosilane precursors exhibited high reactivity toward nucleophilic substitution¹⁴ and reasonably efficient reactions involving proton abstraction. Reactions 5 and 6, which are of the type described by DePuy,¹⁵ involved displacement reactions by fluoride ion on substituted disilanes. Such nucleophilic displacement reactions were the preferred method for silyl anion generation. In general, best signals were obtained using 1×10^{-7} Torr of NF_3 (MeOOME) and 3×10^{-7} Torr of the appropriate organosilane. For reactions 5/5a, MeSiH_2^- and Me_2SiH^- ions were observed in a ratio of 2:1. For reactions 7/7a/7b, PhMeSiH^- , MeHSiF^- and C_6H_5^- were observed in a ratio of approximately 2.5:1.5:1.0. Since reaction 7/7a/7b gives addition-elimination products, we attempted to generate PhMeSiH^- from 1,2-dimethyl-1,2-diphenylsilane. The low vapor pressure of this reagent, however, made this approach unfeasible.

Instrumental. Data acquisition in the equilibrium experiments was performed in the following manner. The ICR was operated in a pulsed mode¹⁶ in which repetitive cycles of ion generation, reaction, detection, and removal from the cell were carried out, enabling the measurement of ion concentrations as a function of time with millisecond resolution. Ion signals from the capacitance bridge detector were channeled into a boxcar averager (operated as a sample and hold) and then to either an XY recorder or IBM PC. The microcomputer was used to process signals as well as to control the timing circuitry during the experiment.¹⁷

The equilibrium constant between the two acids and their conjugate bases in eq 1 can be obtained from the ratio of the forward and reverse rate constants. Rate constants for the forward reaction were measured by ejecting R_3Si^- using double resonance techniques¹⁸ and monitoring the decrease of A^- in the presence of R_3SiH . Since the neutral concentration was much greater than the ion concentration, the disappearance of A^- is pseudo-first-order. Rate constants were obtained by dividing the slope of straight line plots [\ln (fractional decrease) versus time] by the R_3SiH pressure. Reverse rate constants for (1) were obtained in an analogous manner by ejecting A^- . Rate constants for the alcohol-organosilane thermoneutral reactions were roughly encounter controlled.

Equilibrium constants, in most cases, were also obtained from measurements of relative equilibrium abundances of ions and the relative neutral gas pressures, as shown in eq 10.

$$K = (\text{R}_3\text{Si}^-)(\text{AH})/(\text{A}^-)(\text{R}_3\text{SiH}) \quad (10)$$

Pressure measurements in both cases were obtained using a Varian UHV-24 ionization gauge, which was itself calibrated using an MKS Baratron capacitance manometer and checked against the rate constant measurements of the methane/methane cation proton-transfer reaction. The ratio of ion concentrations was obtained from the ratio of peak heights in a mass scan of each ion (frequency scan at constant magnetic field) after the ions had reached equilibrium. Equilibrium was observed with time scans and verified by double resonance ejection.

Error bars on the equilibrium constants reflect the variation of the measured rate constants for ion disappearance over sets of runs at dif-

(6) Reed, K. J.; Brauman, J. I. *J. Chem. Phys.* **1974**, *61*, 4830.

(7) Nimlos, M. R.; Ellison, G. B. *J. Am. Chem. Soc.* **1986**, *108*, 6522.

(8) Walsh, R. *Acc. Chem. Res.* **1981**, *14*, 246.

(9) Circuitry development reported in: McIver, R. T., Jr.; Hunter, R. L.; Ledford, E. B., Jr.; Locke, M. J.; Francl, T. J. *Int. J. Mass. Spectrom. Ion Phys.* **1981**, *39*, 65.

(10) Performance analysis showing linear response with ion concentration: McIver, R. T., Jr.; Ledford, E. B., Jr.; Hunter, R. L. *J. Chem. Phys.* **1980**, *72*, 2535.

(11) Norman, A. D.; Webster, J. R.; Jolly, W. L. *Inorg. Synth.* **1968**, *11*, 170.

(12) Durig, J. R.; Hellams, K. L.; Mulligan, J. H. *Spectrochim. Acta* **1972**, *28A*, 1039.

(13) Dodd, J. A. Ph.D. Thesis, Stanford University, 1985, p 20.

(14) Consistent with the reactivity of silicon compounds in solution. See: Paquette, L. A. *Science* **1982**, *217*, 793.

(15) DePuy, C. H.; Bierbaum, V. M.; Flippin, J. J.; Grabowski, G. K.; Schmitt, R. J.; Sullivan, S. A. *J. Am. Chem. Soc.* **1980**, *102*, 5012.

(16) For a description of the apparatus used in these laboratories for kinetic measurements, see: Moylan, C. R.; Jasinski, J. M.; Brauman, J. I. *J. Am. Chem. Soc.* **1985**, *107*, 1934.

(17) Barfknecht, A. T. Ph.D. Thesis, Stanford, 1985, Chapter 2.

(18) Anders, L. R.; Beauchamp, J. L.; Dunbar, R. C.; Baldeschwieler, J. D. *J. Chem. Phys.* **1966**, *45*, 1062.

Table I. Equilibrium Measurements^a for Organosilanes (kcal/mol)

R ₃ SiH	AH	ΔG ^o _{acid,298} (AH) ^b	method ^c	K _e	ΔG ^o ₃₅₀ (eq 1)
Me ₃ SiH	CH ₃ OH	374.8	1 ^d		
MeSiH ₃	<i>i</i> -PrOH	369.3	1,2	0.3 ± 0.1	+0.8
PhMeSiH ₂	<i>t</i> -BuC(Me)HOH	365.9	1,2	0.6 ± 0.1	+0.4
SiH ₄	<i>t</i> -BuC(Et)HOH	364.8	1,2	1.7 ± 0.4	-0.4
PhSiH ₃	<i>t</i> -BuC(<i>i</i> -Pr)HOH	363.7	1	5.4 ± 1	-1.2

^aR₃SiH + A⁻ = R₃Si⁻ + AH, 350 K (std state = 1 atm, 298 K). ^bSee text. ^cMethod 1 = kinetic rate constants; method 2 = equilibrium abundances. ^dSee text. ΔG^o_{acid} ≈ ΔG^o_{acid}(CH₃OH).

Table II. Acidities, Electron Affinities, and Si-H Bond Energies (kcal/mol)

R ₃ SiH	ΔG ^o _{acid,298}	ΔH ^o _{acid}	ΔS ^o _{acid}	EA(R ₃ Si ⁺)	D ^o (R ₃ Si-H)
Me ₃ SiH	≥375.0 ± 2	≥382.8 ± 2 (383 ± 3) ^a	24.4	22.4 ± 0.6	≥91.0 ± 2 (90.3 ± 1.4) ^b
MeSiH ₃	370.4 ± 2	378.3 ± 2 (383 ± 3) ^a	26.6	27.5 ± 0.8	92.2 ± 3 (89.6) ^b
PhMeSiH ₂	366.5 ± 2	374.2 ± 2	25.8	30.7 ± 0.9	91.3 ± 3
SiH ₄	364.7 ± 2	372.8 ± 2 (371 ± 2) ^c (371.5 ± 2) ^d	27.2	32.4 ± 0.6 (32.4 ± 0.3) ^c	91.6 ± 2 (90.3 ± 1.2) ^b
PhSiH ₃	362.8 ± 2	370.7 ± 2 (370 ± 3) ^a	26.6	33.1 ± 0.1	90.2 ± 2 (89.3 ± 1.2) ^b

^aReference 5. ^bReference 8. ^cReference 7. ^dReference 1a.

ferent pressures (±10%) and the variation in the pressure calibration (typically ±20%) or the variation between equilibrium constants measured by the different methods. Because the organosilane acidities were obtained from proton-transfer equilibria involving reference alcohol acids, the limiting error associated with the reported silane acidities is not determined by the uncertainty in the equilibrium constant measurements but rather by the absolute error of the reference alcohol acidities (±2 kcal/mol).

Photodetachment experiments were performed using the ICR in a drift mode¹⁹ in which ions were continuously generated and detected. Enhancement of the signal-to-noise ratio by a factor of 100 compared to pulsed mode (due to the proportional amount of detection time) enabled small changes in ion concentration (ca. <0.5%) to be measured. Anion concentrations were measured before and after irradiation; fractional changes at each wavelength were converted to relative electron detachment cross sections^{1b,20} after normalization of photon intensity. A MINC PDP-11/23 laboratory computer (Digital Equipment) or an IBM-XT controlled spectral scans, tuning the wavelength and monitoring the ion signal and photon flux (amplified output of Epply thermopile). For such automated data acquisition, use of detection frequency controlling circuitry²¹ (which ensures that the detection frequency always corresponds to the resonant cyclotron frequency of the ions being monitored) was essential.

Light Sources. Two photon sources were utilized for the photodetachment experiments. A 1000-W xenon arc lamp (Canrad-Hanovia), used in conjunction with a 0.25-m high-intensity monochromator (Kratos Analytical) and appropriate gratings, provided light from 280 to 1400 nm. Spectral bandwidth was varied by selection of slits. In order to obtain sufficient photon fluxes for reproducibly measurable changes in ion concentrations, spectral bandwidths were typically 50 nm (fwhm) in the 800–1400-nm regions (ca. 400 cm⁻¹). Output from an argon ion-pumped dye laser (Innova-15 and Model 590, Coherent Radiation) provided light from 700 to 900 nm (using Exciton dyes LDS 700, 750, and 821). Spectral bandwidth, determined by a three-plate birefringent tuner, was 0.1 nm (ca. 1 cm⁻¹).

Error bars associated with the determination of an onset arise from the ability to determine a change in cross section (dependent on the ΔE between data points and the amount of noise for a particular system) and the spectral bandwidth. The accuracy of the wavelength calibration (±20 cm⁻¹ for the arc lamp and ±1 cm⁻¹ for the dye laser) was not the limiting source of uncertainty.

Results and Analysis

Equilibria Data. Acidities for the organosilanes were derived from the proton-transfer equilibrium constants. Because the

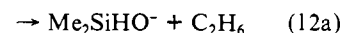
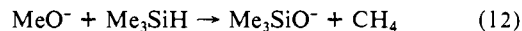
equilibrium proton transfer reactions involved reference acids whose free energies of heterolytic dissociation, ΔG^o_{acid}(AH), are known, the ΔG^o_{acid} for the organosilane acids can be calculated, as shown:

$$\Delta G^{\circ}_{\text{acid}}(\text{R}_3\text{SiH}) = -RT \ln K_e + \Delta G^{\circ}_{\text{acid}}(\text{AH}) \quad (11)$$

Measured equilibrium constants at 350 K corresponding to the reaction as written in eq 1 are contained in Table I along with ΔG^o_{acid,298} for the appropriate reference compounds.^{22,23} The reference values chosen are based on bond energies and electron affinities of methanol and isopropyl alcohol^{22,23a} with the more acidic alcohols referenced to isopropyl alcohol as measured in the original work.^{23b} The values of ΔS^o_{acid} for all of the alcohols are taken²³ as 22 cal deg⁻¹ mol⁻¹ so that ΔG^o_{acid,350} will be 1.1 eu less positive than ΔG^o_{acid,298} for each of these references.

The values of ΔS^o_{acid} for the organosilanes uncorrected for symmetry are taken as 24.4 cal deg⁻¹ mol⁻¹. This value is consistent with entropy changes for similar acids^{23a} and gives a value for ΔS_{acid} for silane (corrected for symmetry) equal to that obtained using entropies of formation of SiH₄, H⁺, and PH₃ as an isoelectronic analogue of SiH₃⁻. The values of ΔG^o_{acid}, ΔH^o_{acid}, and ΔS^o_{acid} for the organosilanes are listed in Table II. Agreement with the results of Damrauer, Kass, and DePuy⁵ is quite good except for MeSiH₃. Following the publication of Damrauer et al.,⁵ we reconfirmed by FT-ICR and double resonance experiments that the reaction between MeSiH₂⁻ and *i*-PrOH is reversible.

The acidity measurement in the proton-transfer reaction between trimethylsilyl anion and methanol is complicated by the competition of another reaction channel. It was not possible to measure an equilibrium constant, because methoxide reacts with trimethylsilane as shown:²⁴



Thus, the Si-H acidity reported for trimethylsilane must be set as less than or equal to that for MeOH. Based on the derived

(19) For a general description of ICR as used in these laboratories for spectroscopy experiments, see: Wetzel, D. M.; Brauman, J. I. *Chem. Rev.* **1987**, *87*, 607.

(20) Determination of relative cross section from fractional signal changes relies on the steady-state model description of ion behavior in the ICR, as discussed by: Zimmerman, A. H., Ph.D. Thesis, Stanford, 1977, p 13.

(21) Marks, J.; Drzaic, P. S.; Foster, R. F.; Wetzel, D. M.; Brauman, J. I.; Uppal, J. S.; Staley, R. H. *Rev. Sci. Instrum.* **1987**, *58*, 1460.

(22) Moylan, C. R.; Brauman, J. I. *J. Phys. Chem.* **1984**, *88*, 3175. Essentially the same value for the acidity of methanol has been determined by Mautner and Sieck from equilibrium measurements: Meot-Ner (Mautner), M.; Sieck, L. W. *J. Phys. Chem.* **1986**, *90*, 6687.

(23) (a) Lias, S. G.; Bartmess, J. E.; Holmes, J. L.; Levin, R. D.; Liebman, J. F.; Mallard, W. G. *Gas Phase Ion and Neutral Thermochemistry*, *J. Phys. Chem. Ref. Data*, **1988**, *17*, Suppl. 1. (b) Bartmess, J. E.; Scott, J. A.; McIver, R. T., Jr. *J. Am. Chem. Soc.* **1979**, *91*, 6047.

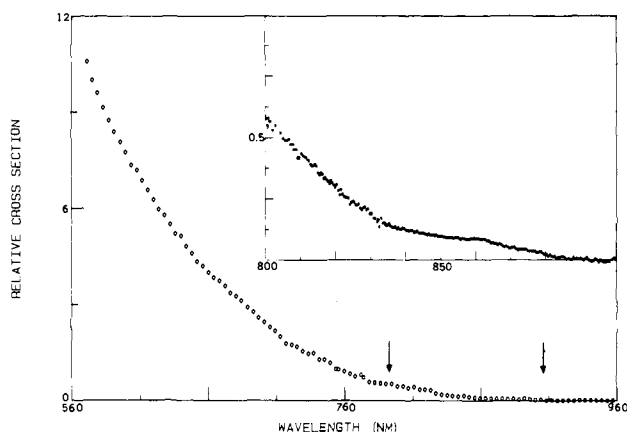


Figure 1. Low-resolution photodetachment spectrum of SiH_3^- (bandwidth = 58 nm fwhm). High-resolution data (0.1 nm) in the region indicated by arrows shown in the inset.

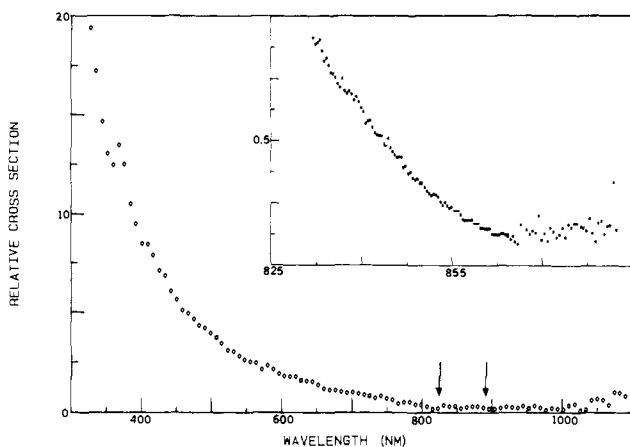


Figure 2. Low-resolution photodetachment spectrum of PhSiH_2^- (bandwidth = 58 nm fwhm). High-resolution data (0.1 nm) in the region indicated by arrows shown in the inset.

bond dissociation energy and the consistency with measurements made by completely different methods, however, we believe the true Si-H acidity to be very close to that of MeOH.

Bowie and co-workers had previously studied the reaction between methoxide ion and trimethylsilane,²⁴ and observed trimethylsiloxide ion to be the major reaction product. In addition, however, they detected small amounts of deprotonation product. Based on the results of deuterium labeling experiments, Bowie and co-workers reported deprotonation exclusively at carbon.

If MeO^- were responsible for this deprotonation, then the C-H acidity must be comparable to the Si-H acidity, namely, $\Delta H^\circ_{\text{acid}} \approx 380$ kcal/mol. A C-H acidity of this magnitude is difficult to rationalize when compared to the C-H acidity in tetramethylsilane,²⁵ $\Delta H^\circ_{\text{acid}} = 390.9 \pm 1.5$ kcal/mol. It suggests that the removal of one β methyl group enhances the C-H acidity by 10 kcal/mol, a rather large and unprecedented effect. The results of the organosilane acidity bracketing experiments by Damrauer, Kass, and DePuy⁵ (which indicated that the C-H acidity in methylsilane is approximately 390 kcal/mol) also indicate that deprotonation by MeO^- is not probable.

Under our conditions, when MeO^- (prepared from low-energy electron capture on MeOOMe) was allowed to react with trimethylsilane, we observed Me_3SiO^- , Me_2HSiO^- and $\text{Me}_3\text{HSiOMe}^-$ but no deprotonation products (<1%). The total pressure in the Bowie experiment was 10^{-5} Torr. In our apparatus, poor ion trapping at pressures higher than 10^{-6} Torr precluded reproduction of the Bowie conditions. Since we do not observe deprotonation

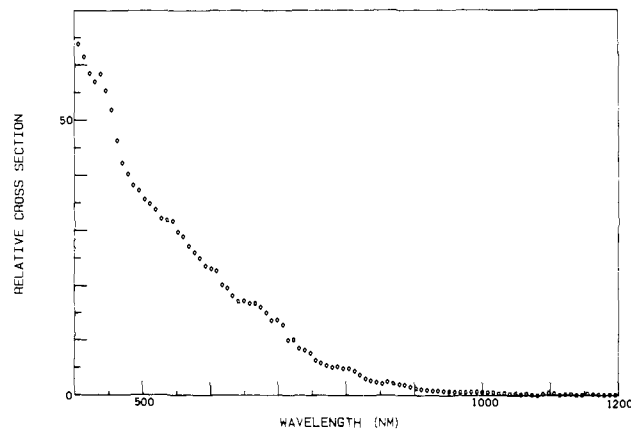


Figure 3. Photodetachment spectrum of PhMeSiH^- (bandwidth = 51 nm fwhm).

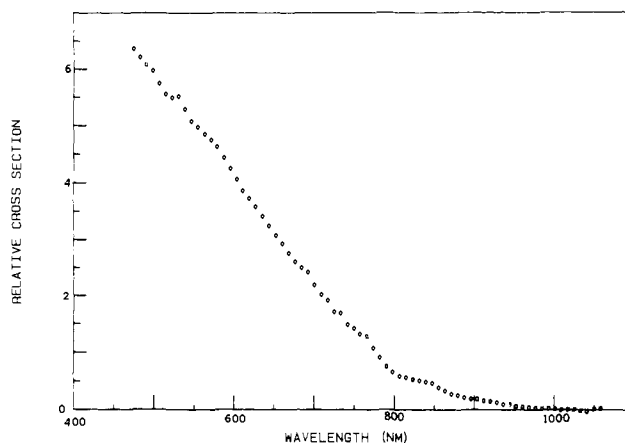


Figure 4. Photodetachment spectrum of MeSiH_2^- (bandwidth = 51 nm fwhm).

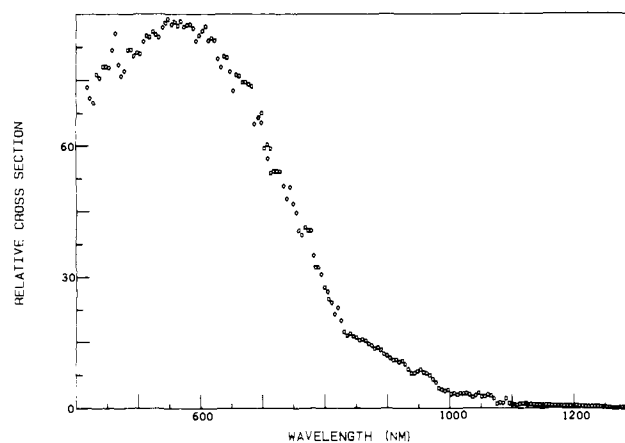


Figure 5. Photodetachment spectrum of Me_3Si^- (bandwidth = 51 nm fwhm).

products in our experiments, which are conducted at lower pressures, it is possible that deprotonation occurs via a secondary reaction.

We would expect deprotonation at carbon to be accomplished only by a strongly basic ion, consistent with observations by Damrauer et al.⁵ A possible deprotonating base could be hydride ion, generated in the decomposition^{3,26} of the pentacoordinate silicon anion, $\text{Me}_3\text{HSiOMe}^-$, formed in eq 12b.

Photodetachment Data. The photodetachment spectra of the five organosilyl anions are displayed in Figures 1-5. The spectra consist of data collected over the 300-1200-nm region using

(24) Klass, G.; Trenerry, V. C.; Sheldon, J. C.; Bowie, J. H. *Aust. J. Chem.* **1981**, *34*, 519.

(25) Wetzel, D. M.; Brauman, J. I. *J. Am. Chem. Soc.* **1988**, *110*, 8333.

(26) Tumas, W.; Salomon, K. E.; Brauman, J. I. *J. Am. Chem. Soc.* **1986**, *108*, 2541.

low- and high-resolution light sources, as indicated in the figure captions.

Three features of the photodetachment spectra are common to all five anions. In all spectra the first onset occurs in the near-IR region at wavelengths greater than 850 nm. In addition, the cross-section curves in this threshold region are very shallow, rising slowly with increasing energy. Finally, all spectra also exhibit cross-section behavior to the blue of the threshold region that is dramatically different from the cross-section behavior at threshold. The cross sections at approximately 750 nm are at least a factor of 10 larger than the cross sections near threshold and begin to rise much more rapidly as a function of increasing energy. This difference in cross-section behavior suggests that transitions other than simple continuum photodetachment are being accessed in the optical experiments.²⁷ Transitions to low-lying valence electronic excited states of the anions imbedded in the continuum would exhibit cross-section behavior such as that observed in the organosilyl detachment spectra. The detachment spectrum of Me_3Si^- , Figure 5, is a particularly distinct example, exhibiting an absorption maximum at approximately 570 nm.

Analysis of the detachment spectra consisted of the determination of transition energies for onsets observed in the spectra and the assignment of these energies to specific transitions between levels of the anion and the neutral. Of particular interest is the transition from the ground rovibrational level of the anion to the ground rovibrational level of the neutral. This transition energy corresponds to the adiabatic electron affinity of the neutral molecule.

Because photodetachment spectroscopy involves bound to continuum transitions, the spectra are integral in nature. Transition energies correspond to the wavelengths at which the cross-section curve changes slope. We provide a brief description of the analysis of each of the photodetachment spectra and the subsequent assignment of the $0 \leftarrow 0$ transition energy.

The high-resolution photodetachment spectrum for silyl anion in the 800–900-nm wavelength region (inset to Figure 1) exhibits two onsets, one occurring at 890 ± 5 nm, the other at 829.5 ± 4.5 nm. The lowest energy onset was determined as that wavelength corresponding to the first nonzero cross section; error bars reflect the uncertainty of assigning a particular data point as a nonzero cross section apart from the noise in the data set. The higher energy onset was determined by examining the first derivative of the data, fit by a smoothed least-squares spline function.²⁸

The experimentally observed onsets do not correspond to the rotationless transition energy between vibrational levels of the anion and neutral and must be corrected for rotational broadening. The extent of rotational broadening can be determined by convoluting the cross section function with the calculated manifold of allowed rotational transitions. We approximated the cross-section function as a step function and calculated the manifold of allowed rotational transitions using the rotational constants obtained in *ab initio* calculations⁷ on SiH_3^- and SiH_3 . Two assumptions were made in calculating the rotational broadening. We included transitions out of J levels constituting 95% of the Boltzmann intensity envelope at 300 K, which assumes that transitions from levels with less than 5% of the total population distribution cannot be reliably detected in our experiment. The calculated rotational manifold shows that 95% of the total intensity lies in a 17 nm wavelength region, from wavelengths 7 nm longer than, to 10 nm shorter than the wavelength of the rotationless transition. We assumed that the rotational broadening is 17 nm, and subtracted one-half the rotational manifold (8.5 nm) from the experimentally observed onsets. Thus, the transition energies corresponding to the rotationless transition between vibrational levels of the anion and neutral are assigned²⁹ 1.406 ± 0.028 eV (881.5 nm) and 1.510 ± 0.030 eV (821 nm).

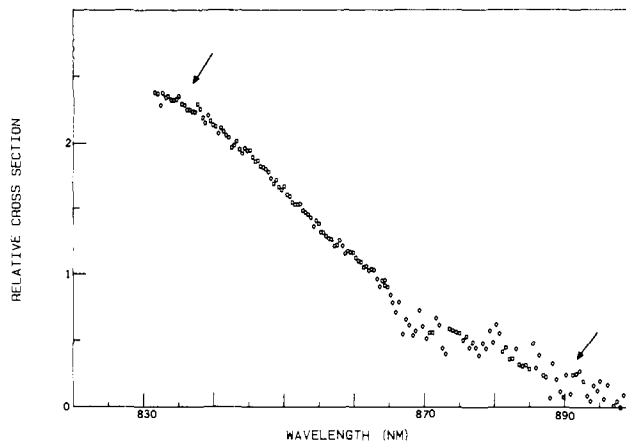


Figure 6. High-resolution (0.1 nm) photodetachment spectrum of SiD_3^- . Arrows indicate positions of the onsets observed in the high-resolution detachment of SiH_3^- .

In order to determine which of these transition energies corresponded to the $0 \leftarrow 0$ transition, the photodetachment spectrum of SiD_3^- was recorded (Figure 6). Exchange of hydrogens for deuterium is not expected to change the $0 \leftarrow 0$ transition energy significantly. Transitions to higher vibrational levels of the neutral, however, will occur at different energies (wavelengths) in the hydride and deuteride spectra. Transitions from the ground vibrational level in the anion to excited vibrational levels in the neutral will occur at lower energies (longer wavelengths) in the deuteride, reflecting the difference in vibrational frequencies of the deuteride and hydride. Two onsets occur in the detachment spectrum of SiD_3^- , assigned at 896 ± 8 and 865 ± 5 nm (Figure 6). The arrows in Figure 6 indicate the wavelengths at which the two SiH_3^- onsets occur. Because the higher energy transition shifted to lower energy by 35 nm (over 400 cm^{-1}) and the lower energy transition shifted by 6 nm (less than 100 cm^{-1}) upon deuterium substitution, we assign the lower energy transition at 881.5 nm as the energy of the $0 \leftarrow 0$ transition and thus the electron affinity of SiH_3^* .

The off-diagonal transition is the more intense feature in the silyl anion detachment spectrum, indicating that a geometry change occurred in going from the anion to the neutral. Our observations are consistent with photoelectron spectroscopy results⁷ and *ab initio* calculations.³⁰

The high-resolution photodetachment data for PhSiH_2^- (inset to Figure 2) indicate an onset occurring at 865 ± 2 nm. The calculated rotational broadening in this anion is small, approximately 2 nm; thus the onset was determined to occur at 864 ± 2 nm. As can be seen in both the high- and low-resolution data, a nonzero cross section was observed well into the near-IR. Low-resolution data indicated that this cross section approaches zero at approximately 960 nm.

Because the data suggested the presence of two onsets, the photodetachment spectrum of PhSiD_2^- was recorded in the 800–900-nm region. We expected the onset at 864 nm to shift either by less than 100 cm^{-1} for the $0 \leftarrow 0$ transition or by over 300 cm^{-1} for the $1 \leftarrow 0$ transition. The data acquired for the deuterated anion did not provide conclusive results: no onsets could be assigned in the wavelength region scanned, and red shifts to energies greater than 300 cm^{-1} would fall outside the range of photon energies accessible to an argon ion-pumped dye laser. Without more conclusive data similar to that obtained in the silyl anion experiment, we were hesitant to assign the onset at 864 nm as the $1 \leftarrow 0$ transition, and we thus assign it as the $0 \leftarrow 0$ transition. Any nonzero cross section to the red of 865 nm is therefore either a hot band transition³¹ or due to heating effects

(27) Zimmerman, A. H.; Gyax, R.; Brauman, J. I. *J. Am. Chem. Soc.* **1978**, *100*, 4766.

(28) Janousek, B. K.; Zimmerman, A. H.; Reed, K. J.; Brauman, J. I. *J. Am. Chem. Soc.* **1978**, *100*, 6142.

(29) As the functional form of the cross section is not known, the error bars reflect the uncertainty due to rotational broadening.

(30) (a) Calculations on the anion: Eades, R. A.; Dixon, D. A. *J. Chem. Phys.* **1980**, *72*, 3309. (b) Calculations on the radical: Bunker, P. R.; Olbrich, G. *Chem. Phys. Lett.* **1984**, *109*, 41.

in the ICR.³² Assignment of the $0 \leftarrow 0$ transition energy at 864 nm is ultimately rationalized by the agreement between the resulting thermochemical parameters and existing literature values. The other assignment is less satisfactory.

Transition energies for PhMeSiH^- , MeSiH_2^- , and Me_3Si^- (Figures 3–5) were assigned from detachment data taken at low resolution with the arc lamp, since the lowest energy onsets occurred at longer wavelengths than those accessible using argon ion-pumped dye lasers. Onsets were obtained from linear extrapolation of the low-resolution data and a correction of one-half the fwhm (=25 nm). In all three cases, error bars associated with the measured transition energy reflect both the uncertainty in assigning the nonzero cross section and the experimental bandwidth; rotational corrections fell well within these limits.

For PhMeSiH^- (Figure 3), linear extrapolation of the data results in an observed onset at 955 nm. Subtraction of one-half fwhm, 25 nm, results in a threshold of 930 ± 30 nm, which was assigned as the $0 \leftarrow 0$ transition. A small cross section for photodetachment was observed to the red of this onset. As in the PhSiH_2^- case, these cross sections are attributed to either hot bands or thermal effects.³²

For MeSiH_2^- and Me_3Si^- (Figures 4 and 5), the observed onsets were at 1065 and 1300 nm, respectively. Correction for the monochromator bandwidth results in threshold assignments of 1040 ± 30 and 1275 ± 30 nm, respectively.

Table II lists the $\Delta G^\circ_{\text{acid},298}$, $\Delta H^\circ_{\text{acid}}$, and $\Delta S^\circ_{\text{acid}}$ values for the organosilanes obtained from the equilibria experiments as well as the electron affinities obtained from analysis of the photodetachment spectra. In addition, homolytic bond dissociation energies, obtained from the electron affinities and acidities³³ are shown. The thermochemical parameters appearing within parentheses in Table II are literature values, included for comparison. The agreement of the bond dissociation energies with those measured independently supports the assumptions made in the assignment of the photodetachment onsets as well as the acidity measurements.

The detachment spectrum of Me_3Si^- permitted assignment of the transition energy to an excited electronic state of the anion. The observed $\lambda_{\text{max}} = 570 \pm 25$ nm places the electronic state approximately 2.2 eV above the ground state of the anion.

Discussion

The data obtained for the organosilane systems indicate some remarkable features in the energetics and electronic structure of silicon-containing molecules. The magnitudes of the electron affinities indicate the stability of organosilyl anions. Trends in the acidity and electron affinity data reflect alkyl- and aryl-substituent effects in silyl anion. The bond dissociation energies provide information about the effects of hybridization in neutral organosilanes and organosilyl radicals, and indicate relative stabilities of the organosilyl radicals.

Bond Energies and Radical Stabilities. As seen from the data in Table II, the Si–H bond dissociation energy is about 90 kcal/mol for all the organosilanes included in this study. Unlike carbon, silicon–hydrogen bond dissociation energies do not appear to be sensitive to alkyl substitution. This reflects the modest geometry and bonding changes on going from neutral silanes to the corresponding silyl radicals. Therefore, different alkyl or aryl groups attached to the silicon do not affect the bond strength. These conclusions are similar to conclusions reached previously

by both Walsh⁸ and Griller and co-workers³⁴ based on their measurements of Si–H bond dissociation energies. The lack of substituent effects in organosilanes is interestingly different from carbon compounds. C–H bond dissociation energies decrease with alkyl substitution,³⁵ reflecting the relative sensitivity in C–H versus C–C bonding on going to the planar radical.

We expect that the organosilane Si–H bond dissociation energies are a measure of radical stabilities, behavior similar to alkanes. The data show that silyl radical stabilities are not affected by alkyl or aryl substitution, as noted previously by Walsh.⁸ Resonance delocalization, important in benzyl radical³⁵ ($D^\circ(\text{CH}_3\text{--H}) = 105.1$ and $D^\circ(\text{C}_6\text{H}_5\text{CH}_2\text{--H}) = 88.0$ kcal/mol), is unimportant in phenylsilyl radical. Since the radical stabilities are unaffected by substitution, the observed trends in the acidity and electron affinity data reflect the stabilities of the organosilyl anions.

Anion Stabilities. The large electron affinities are noteworthy. Organosilyl anions, whether containing hydrogen, alkyl, or aryl substituents, are very stable anions. In this regard, organosilyl anions are dramatically different from analogous aliphatic carbanions, known to be either weakly bound³⁶ or unbound species³⁷ in the gas phase.

A description of the electronic structure of silyl anion rationalizes the experimental observations. Quantitative calculations of atomic population data³⁸ in tricoordinate, pyramidal second-row hydrides (AH_3) indicate decreasing s-orbital contribution to overlap density with decreasing bond angle. The optimized geometry obtained from ab initio calculations on silyl anion^{30a} indicates that the H–Si–H bond angle is 97° . For this geometry the nonbonding electrons are in an orbital with substantial s character.

The functional form of the photodetachment cross section depends strongly on the type of orbital from which the electron is removed. The theory modeling the detachment cross section in polyatomic anions³⁹ predicts an energy dependence of $\sigma(E) \propto \Delta E^{3/2}$ near threshold for detachment from an s orbital. The photodetachment spectra show such cross-section behavior in each individual rovibrational onset observed in the near-IR region. These data therefore also indicate that the “extra” electron resides in an orbital with substantial s character.

A consequence of the electronic structure is that electrons are held more tightly in silyl anions compared with methyl anion, in which the nonbonding electrons are in an almost pure p orbital. Thus silicon, although more electropositive than carbon, is better able to accommodate excess charge. Calculations on methylsilyl and silylmethyl anions⁴⁰ also support this conclusion.

In summary, because of differences in s–p splitting, the lowest energy configuration differs for tricoordinate methyl and silyl anions. In the essentially planar methyl anion, the s orbital is used for C–H bonding, leaving the nonbonding electrons in a p orbital. In the pyramidal organosilyl anions, the electron can be placed in an orbital with substantial s character.

Silyl anion does not appear to be stabilized by resonance delocalization. This can be seen from the acidities and the electron affinity data, $\text{EA}(\text{SiH}_3^*) = 32.4$ and $\text{EA}(\text{PhSiH}_2^*) = 33.1$ kcal/mol. This effect may be due to poor overlap, because of differences in orbital size and less than optimal angular overlap as well as to a possible energy mismatch. In contrast, resonance delocalization is quite important in determining the relative stabilities of the analogous carbanions,³⁶ ($\text{EA}(\text{CH}_3^*) = 1.8$ and⁴¹ $\text{EA}(\text{C}_6\text{H}_5\text{CH}_2^*) = 19.9$ kcal/mol).

(31) Based on the wavelength at which the cross section goes to zero, a hot band vibrational frequency of approximately 1000 cm^{-1} can be obtained. Boltzmann population of this level is not expected to be much greater than 1%, even if the reaction exothermicity (3 kcal/mol, based on the acidity of HF) is converted into PhSiH_2^- internal energy. While the observation of detachment out of this level seems unlikely, it should not be discounted since Franck–Condon factors in silyl systems favor off-diagonal transitions.

(32) In the course of these detachment experiments, PhSiH_2^- and PhMeSiH^- frequently exhibited anomalous thermal effects, such as ion signal increases upon irradiation. Photoincreases indicate that trapping conditions differ with and without photons entering the ICR and make measurements involving small changes in ion concentration problematic.

(33) The thermochemical cycle used to derive bond dissociation energies is $D^\circ(\text{R--H}) = \Delta H^\circ_{\text{acid}}(\text{RH}) + \text{EA}(\text{R}^*) - \text{IP}(\text{H}^*)$; see ref 1a or b.

(34) Kanabus-Kaminska, J. M.; Hawari, J. A.; Griller, D.; Chatgililoglu, C. *J. Am. Chem. Soc.* **1987**, *109*, 5267.

(35) Golden, D. M.; McMillan, D. F. *Annu. Rev. Phys. Chem.* **1982**, *33*, 493.

(36) Ellison, G. B.; Engelking, P. C.; Lineberger, W. C. *J. Am. Chem. Soc.* **1978**, *100*, 2556.

(37) Graul, S. T.; Squires, R. R. *J. Am. Chem. Soc.* **1988**, *110*, 607.

(38) Magnussen, E. *J. Am. Chem. Soc.* **1984**, *106*, 1177.

(39) (a) Reed, K. J.; Zimmerman, A. H.; Andersen, H. C.; Brauman, J. I. *J. Chem. Phys.* **1976**, *64*, 1368. (b) Engelking, P. C. *Phys. Rev. A* **1982**, *26*, 740.

(40) Hopkinson, A. C.; Lien, M. H. *J. Org. Chem.* **1981**, *46*, 998.

(41) Drzagic, P. S.; Brauman, J. I. *J. Phys. Chem.* **1984**, *88*, 5285.

The changes in silyl radical electron affinities and silane acidities with methyl substitution reveal a modest destabilization effect. Methyl groups lower the electron affinities of the radicals and decrease the acidities of the silanes, evidence for destabilization of the silyl anion. Phenyl does not show such destabilization.

Experimental results and theoretical investigations involving neutral organosilanes are pertinent to understanding the interactions involved in the observed methyl destabilization of silyl anions. Michl and co-workers,⁴² in an investigation of electronic perturbations caused by substituents on benzene, such as $-\text{SiH}_3$, $-\text{SiH}_2\text{Me}$, $-\text{SiHMe}_2$, and SiMe_3 , using magnetic circular dichroism (MCD) spectroscopy, found evidence for π -electron donation from methyl to silicon. The π -acceptor ability of a SiH_3 substituent was observed to decrease with successive replacements of Me for H. These MCD experimental results were rationalized within the framework of perturbational molecular orbital theory: the filled, π -type bonding orbitals of the methyl group donate electron density to the unfilled, π -type antibonding orbitals of silicon. Another way to describe the interaction is back-bonding from the C-H bonding orbitals of the methyl group to the Si-H or Si-C antibonding orbitals. This results, in part, from the electropositive nature of silicon which causes the bonding Si-R(H) orbitals to have large coefficients on R(H) and the antibonding orbitals to have large coefficients on Si.

Calculations indicate this net $C_\pi \rightarrow \text{Si}_\pi^*$ electron donation is important in silaethane⁴³ and also occurs in methyl silyl anion.^{40,44,45} In the silyl anion, however, where the excess charge resides predominantly on the silicon atom, this net electron-donating interaction is destabilizing. With respect to the radical, the relative stabilities of SiH_3^- , MeSiH_2^- , and Me_2SiH^- and those of PhSiH_2^- and PhMeSiH^- are consistent with this description. The effect

(42) Weeks, G. H.; Adcock, W.; Klingensmith, K. A.; Waluk, J. W.; West, R.; Vasak, M.; Downing, J.; Michl, J. *Pure Appl. Chem.* **1986**, *58*, 39.

(43) Bernardi, F.; Bottoni, A.; Tonachini, G. *Theor. Chim. Acta* **1979**, *52*, 37.

(44) Hopkinson, A. C.; Lien, M. H. *Tetrahedron* **1981**, *37*, 1105.

(45) For an experimental determination of the stabilization of carbanions by α -silyl groups, see ref 25.

of methyl substitution on the anion stability is not additive, but appears to show saturation.

The photodetachment spectra give evidence for low-lying (ca. 2 eV) valence electronic states in trimethylsilyl anion. The rapid increase in the cross sections of the other anions suggests that they also have low-lying electronic states, although the maxima are beyond the range of our data. The effect of methyl groups in raising the orbital energy of the nonbonding electrons appears here also, with trimethylsilyl anion having its transition at an energy lower than the corresponding one in the other anions. The excited state very likely involves a Si-R antibonding orbital. This orbital is expected to have a large contribution (large coefficient) on silicon.

Conclusions

We have measured gas-phase equilibrium constants and electron photodetachment onsets for a series of alkyl- and aryl-substituted silyl compounds and report the resultant acidities, electron affinities, and bond dissociation energies. The data indicate that (1) silyl anions are quite stable, (2) methyl groups cause modest destabilization in organosilyl anions, (3) resonance delocalization appears to be unimportant in stabilizing silyl anions, and (4) substitution and geometry changes in organosilyl anions and radicals are relatively unimportant.⁴⁶

Acknowledgment. We are grateful for support by the National Science Foundation, and materials made available by the San Francisco Laser Center, supported by the National Science Foundation. We thank Professors J. Michl, G. B. Ellison, and R. Damrauer for helpful discussions.

Registry No. Me_3SiH , 993-07-7; MeSiH_3 , 992-94-9; PhMeSiH_2 , 766-08-5; SiH_4 , 7803-62-5; PhSiH_3 , 694-53-1; Me_2Si^* , 16571-41-8; MeSiH_2^* , 51220-22-5; PhMeSiH^* , 119946-89-3; SiH_3^* , 13765-44-1; PhSiH_2^* , 72975-30-5.

(46) **Added in Proof:** See Gordon, Boatz, and Walsh (Gordon, M. S.; Boatz, R. J. *Phys. Chem.* **1989**, *93*, 1484) for a discussion of additivity in silane heats of formation.

Reactions of Methanol Clusters following Multiphoton Ionization

S. Morgan, R. G. Keese, and A. W. Castleman, Jr.*

Contribution from the Department of Chemistry, The Pennsylvania State University, University Park, Pennsylvania 16802. Received June 3, 1988

Abstract: Clusters of methanol formed in a supersonic expansion are subjected to multiphoton ionization (MPI) at 266 nm using a pulsed Nd:YAG laser. The resulting cluster ions, $\text{H}^+(\text{CH}_3\text{OH})_n$, are found to undergo several intracluster reaction pathways which display a dependence on the degree of aggregation. In addition to the evaporation loss of methanol monomers at all sizes, and the loss of H_2O from the protonated dimer, it is found that a channel corresponding to $(\text{CH}_3)_2\text{O}$ and CH_3OH loss, with H_2O retention, also occurs. For clusters comprised of four to nine methanol molecules, the $(\text{CH}_3)_2\text{O}$ elimination is observed to take place over the time window of about 1 to 15 μs after ionization, while prompt $(\text{CH}_3)_2\text{O}$ elimination also occurs in the size range above $n = 7$. The mechanisms are considered in terms of estimated energetics for the various pathways.

Under certain conditions following the ionization of a cluster, reactions proceed between various moieties within the cluster ion that in terms of products often parallel bimolecular gas-phase ion-molecule reactions. Several examples have been reported in the literature for systems comprised of both hydrogen-bonded clusters as well as ones stabilized by weaker van der Waals dispersion forces.¹⁻⁴

Clusters comprised of methanol molecules represent a promising system for exploring reactions as a function of cluster size. Reactions between methanol ions and methanol have been well explored in the gas phase by both ICR⁵ and fast-flow reactor

(2) Echt, O.; Dao, P. D.; Morgan, S.; Castleman, A. W., Jr. *J. Chem. Phys.* **1985**, *82*, 4076.

(3) Garvey, J. F.; Bernstein, R. B. *J. Am. Chem. Soc.* **1987**, *109*, 1921.

(4) Stephan, K.; Futrell, J. H.; Peterson, K. I.; Castleman, A. W., Jr.; Mark, T. D. *J. Chem. Phys.* **1982**, *77*, 2408.

(1) Klots, C. E.; Compton, R. N. *J. Chem. Phys.* **1978**, *69*, 1644.